Direct Fluorination of Twaron Fiber and Investigation of Mechanical Thermal and Morphological Properties of High Density Polyethylene and Twaron Fiber Composites

J. Maity,[1] C. Jacob,[1] C. K. Das,[1] R. P. Singh[2]

[1]*Materials Science Centre, Indian Institute of Technology, Kharagpur 721302, India*
[2]*University of Lucknow, Lucknow 226007, India*

Received 8 June 2007; accepted 28 August 2007
DOI 10.1002/app.27510
Published online 6 December 2007 in Wiley InterScience (www.interscience.wiley.com).

ABSTRACT: Composites consisting of high density polyethylene (HDPE) reinforced with randomly oriented chopped Twaron fibers (both fluorinated and nonfluorinated) show a significant increase in mechanical and thermal properties. To increase the better fiber matrix adhesion, the Twaron fiber is surface fluorinated using elemental fluorine. The surface of the Twaron fiber becomes very rough and the diameter of Twaron fiber increases from $\sim$ 12 to 14 μm after fluorination. The composites were prepared using solution method to overcome the damage of the fiber. The tensile strength and the Young's modulus increases with increasing fiber content. The tensile strength and modulus of modified fiber (fluorinated Twaron fiber) composites is much higher than nonmodified fiber composites indicating that there is better mechanical interlocking between the modified fiber and the matrix. Thermal properties obtained from DSC and DTA-TG analysis of the fluorinated fiber composites are also improved. Contact angle measurements, as well as the surface energy measurements, indicate that the composites are more wettable and is maximum for fluorinated fiber composites i.e., surface energy for fluorinated fiber composites is highest. Crystallinity is also higher for fluorinated fiber composites. © 2007 Wiley Periodicals, Inc. J Appl Polym Sci 107: 3739–3749, 2008

Key words: direct fluorination; chopped fiber composites; contact angle; surface energy; modulus; crystallinity; wettability

INTRODUCTION

Polyolefin's are the low-cost, most widely used, easily processable general polymeric materials. Through blending, filling, and reinforcing, it is possible to obtain high performance of polyolefin-based materials. The interfacial compatibility between the components that affects the performance of composites is the main factor. Usually, the compatibility between polyolefins and other materials is very poor because of hydrophobic and the inert nature of polyolefins. This poor compatibility in the blends often results in bad mechanical properties.

High-performance composite applications require reinforcement by fibrous materials with outstanding mechanical properties. Especially, polymeric fibers, such as poly(*p*-phenylene terephthalamide) (i.e., Kevlar/Twaron fibers) are well suited to high-performance composite applications, because they combine a high specific strength and modulus with a high thermal resistance and chemical inertness, and moreover, they exhibit low electrical conductivity compared with metallic or carbon fibers. Since it came to market in 1972, the availability of Kevlar/Twaron aramid fibers has advanced in material science, particularly in the areas of fiber-reinforced composites, rubber goods, ropes and cables, ballistics, pulp-reinforced friction products, gaskets, and so forth.[1–3] However, the Twaron fiber-reinforced composites show poor interfacial adhesion between the Twaron fiber and the matrix resin, due to the low surface energy and chemically inert surface of the fiber. Therefore, the properties of the composites and their durability with regard to combined moisture and temperature attack are dependent on the interface between the above two components. For this reason, the interfacial adhesion between the fiber and the matrix has been known as a key factor that determines the mechanical interfacial strength of fiber-reinforced polymer matrix composites. To improve the interfacial adhesion of Twaron fiber reinforced composites, extensive studies have been performed.[4–6] Various methods have been developed to improve or modify the affinity between the components. Among the various methods, chemical treatment is one for improving the interfacial adhesion of organic fiber-reinforced composites.[7–9] And many researches have reported that this improved interfacial adhesion

Correspondence to: C. Jacob (cjacob@matsc.iitkgp.ernet.in).
Contract grant sponsor: Defense Research Development Organization, Govt. of India.

Journal of Applied Polymer Science, Vol. 107, 3739–3749 (2008)

TABLE I
Composition of the Composites

Sample name	Wt. of the nonfluorinated Twaron fiber (g)	Wt. of the fluorinated Twaron fiber (g)
HDTW0	00	–
HDTW1	0.25	–
HDTW2	0.50	–
HDTW3	0.75	–
HDTW4	1.00	–
HDTW5	1.50	–
HDTW1F		0.25
HDTW2F		0.50
HDTW3F		0.75
HDTW4F		1.00
HDTW5F		1.50

can increase several mechanical properties of the composites.[10,11] High-energy treatment approaches including plasma, corona charge, and electron beam have been used to improve the polarity (oxygen concentration) on the surface[12] Other method is to graft polar monomers onto polyolefin molecular chains by solution or melt graft polymerization[13–15] These grafting techniques are complex, elaborate, and involve environmental pollution and damage to the apparatus. Furthermore, the residue graft monomers and other auxiliaries will then have negative effects on the thermal, electrical, and mechanical properties of blends.

Direct fluorination of polymeric materials by using elemental fluorine is one of the most effective techniques to modify the polymer surface.[16–21] Direct fluorination and oxy-fluorination have emerged a premier physicochemical surface modification technique, as this process does not need any initiation proceeding at practically appreciable rates at ambient temperatures for exothermic nature of this reaction. Fluorinated polymers possess a set of unique properties such as enhanced mechanical properties, thermal stability, good barrier and membrane properties, printability, and adherence properties. The direct fluorination can be successfully applied to enhance adhesion properties and printability of HDPE, LDPE, polypropylene, ethylene-vinyl acetate copolymers, polyimides, polyethers, ethylene propylene copolymer, butadiene-styrene copolymers, etc.[22–25] The main advantage of direct fluorination is that the bulk properties of the materials remain unchanged only the thin upper layer is modified.

In this present work, we performed surface treatment of Twaron fibers by direct fluorination method using elemental fluorine and composites were prepared by using high density polyethylene (used as a matrix) with Twaron fiber as the reinforcing materials. The Twaron fiber was treated with 20% Fluorine and 80% Helium mixture. The surface of the Twaron fiber after fluorination becomes very rough. Because of increased surface roughness, the fiber when used for composites preparation better mechanical interlocking takes place between the fiber and the matrix. Then we will concentrate on the effect of fluorinated and nonfluorinated short Twaron fiber reinforcement on thermal, mechanical, and crystalline properties and also the effect of fiber loading on the high density polyethylene matrix. Both fluorinated and nonfluorinated Twaron fiber was used to prepare composites.

EXPERIMENTAL

Materials

The Twaron fiber used in this experiment as a reinforcing agent was Twaron-1055 (AKZO). The matrix was high density polyethylene from IPCL, India.

Fluorination of Twaron fiber

Surface fluorination of Twaron fiber was done in a fluorination system fabricated in our laboratory. Fluorination of the fiber was done by treating with (20% F_2 + 80% He) mixture in closed vessels at total mixture pressure of 95.59 KPa and a temperature of

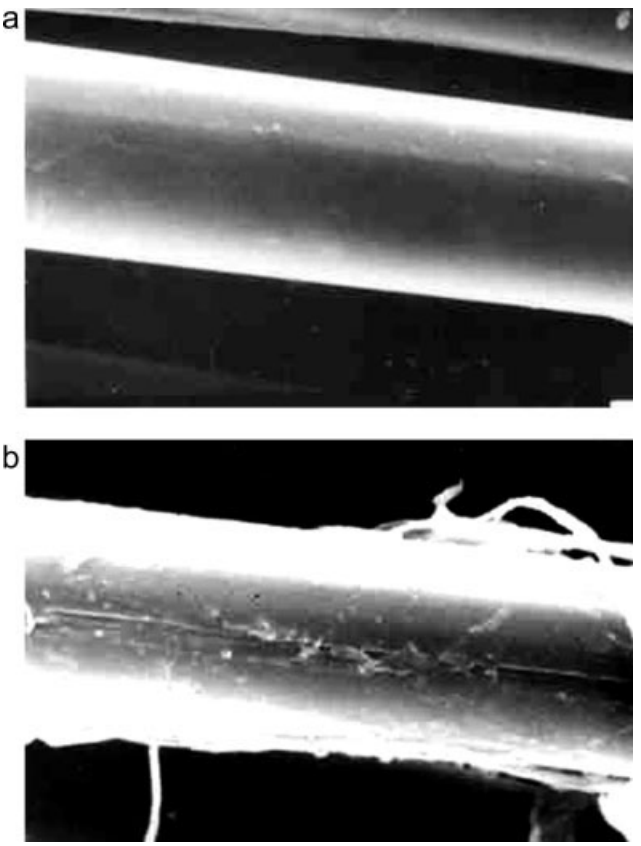

Figure 1 SEM micrograph Twaron fiber (TW) before and (TWF) after fluorination.

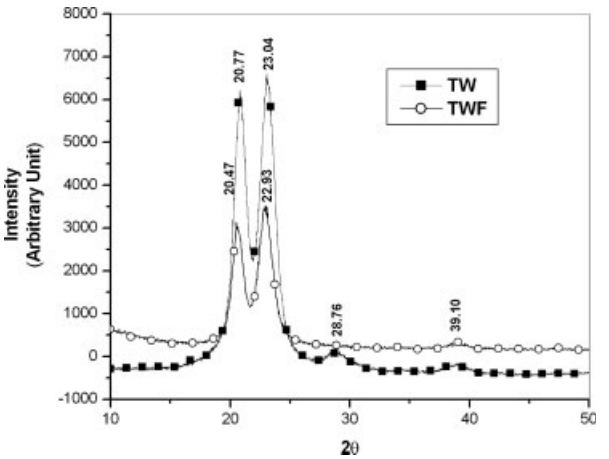

Figure 2 XRD plot of nonfluorinated [TW] fluorinated [TWF] and Twaron fiber.

25°C. The sample was placed inside the reaction chamber and treated for 2 h.

Preparation of composites by solution casting method

The composites were prepared by dissolving the high density polyethylene in toluene at 120°C with continuous stirring. After dissolving the polyethylene a clear solution was obtained. To this clear solution chopped (~ 5 mm length) Twaron fibers (both nonfluorinated and fluorinated fibers) were used in different batches to make the composites. The fibers were added and stirred to distribute the fibers homogeneously. After drying, molding was done in a hot press to get a sheet. The molding condition was 150°C under a pressure of 15 tons. The formulations of the composites are given in Table I.

Mechanical testing

From the molded sheet, dumb-bell-shaped samples were prepared according to ASTM D 424. Tensile testing of the composites was performed at room temperature with a computerized universal testing machine [Hounsfield H25KS Universal Testing Machine (UTM)] at a speed of 5 mm/min.

Scanning electron microscope study

The fibers and the fractured (after tensile testing) samples (composites) were gold coated and their morphology was observed using a scanning electron microscope (SEM) Model No. JEOL JSM 5800 scanning microscope.

X-ray diffraction study

X-ray Diffraction (XRD) of the fibers and composites was carried out by X-ray Diffraction analyzer (Model No: PW 1710 X-ray diffractometer with Cu-target with accelerator (λ = 1.5418 Å) and Ni-filter in the range of 0° to 70° (2θ). The percentage of crystallinity of the sample was then calculated from the analysis of the XRD plot. The percentage of crystallinity was calculated using the following equation. Percent crystallinity = $I_c \times 100/I_c + I_a$, where I_a and I_c are the area under the curve for amorphous and crystalline regions, respectively.[26,27]

IR study

For structural analysis, IR study of the fibers and composites was undertaken using an apparatus, Thermo Nicolet, NEXUS 870 FTIR spectrophotometer. The IR-spectrum was taken in the frequency range of 4000–500 cm^{-1}.

Contact angle measurement

Surface tension (surface free energy) of polymers was tested by contact angle measurements at 24.5°C using a dynamic contact angle measuring instrument (Model No. DCAT II). The single liquid method using distilled water (surface tension 72.75 mN/m) and *N,N*-dimethylformamide (surface tension 37.30 mN/m) as reference liquids was employed. The surface tension (γ) of the polymers was obtained from a combination of the dispersion (γ_d) and polar (γ_p) components of the surface tension $\gamma = \gamma_d + \gamma_p$.

Thermal study

A Perkin–Elmer Pyris Diamond thermo gravimetric analyzer (TGA) (Model No.TG/DTA Perkin–Elmer Instrument. Technology by SII) was used for thermal stability analysis of the virgin matrix and the composites. The prepared sample were scanned between 50 and 650°C under air atmosphere at a heating rate of 10°C/min. Values for onset and ninety percent ($T_{90\%}$) degradation temperature of the samples were determined.

Nonisothermal crystallization kinetics of the composites and virgin matrix were studied by NETZSCH Differential Scanning calorimeter (DSC)

TABLE II
Crystallinity of the Nonfluorinated [TW] and Fluorinated [TWF] Twaron Fiber

Sample name	Crystallinity (%)
Nonfluorinated Twaron fiber (TW)	33.69
Fluorinated Twaron fiber (TWF)	32.81

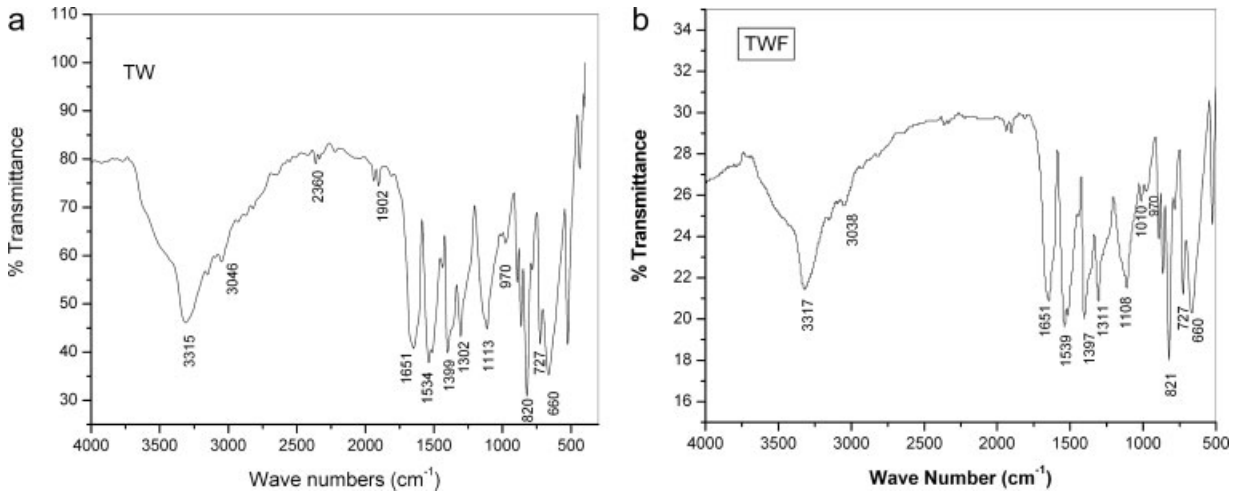

Figure 3 (a) FTIR spectrum of nonfluorinated [TW] Twaron fiber. (b) FTIR spectrum of fluorinated [TWF] Twaron fiber.

(Model No. NETZSCH DSC 200PC) under Nitrogen atmosphere. About 4–5 mg of samples were first heated from −120 to 200°C at a heating rate of 10°C/min. The percentage of crystallinity (X_c) obtained from DSC was determined by using the following relationship.

$$X_c(\%\ \text{crystallinity}) = \Delta H_f \times 100 \,/\, \Delta H_f^0 \times w$$

where ΔH_f and ΔH_f^0 are the enthalpy of fusion of the composites and the enthalpy corresponding to the melting of 100% crystalline HDPE. The value of ΔH_f^0 = 293 J/g was taken for 100% crystalline HDPE[28] and w is the mass fraction of HDPE in the composite.

RESULTS AND DISCUSSIONS

Fiber characterization

The scanning electron micrographs of the fiber before and after fluorination are shown in Figure 1. From SEM image, it can be shown that there is a massive change occurs on the surface. The diameter of the nonfluorinated Twaron fiber was 12 μm, which changes to ~ 14 μm after fluorination. It was also observed from SEM micrograph that after fluorination the fiber surface becomes rough. The increase in surface roughness after the treatment was desirable for improved mechanical interlocking and increased bondable surface area.

The X-ray diffraction plots of the fiber are given in Figure 2. From the XRD plot, the percentage of crystallinity was calculated using the following equation. Percent crystallinity = $I_c \times 100/I_c + I_a$, where I_a and I_c are the area under the curve for amorphous and crystalline regions, respectively. The values (% crystallinity) are given in Table II. From the crystallinity data, it is seen that there is slight change in the crystallinity of fluorinated fiber as compared with the nonfluorinated fibers. Crystallinity of polymer depends on many factors including prevailing physical conditions, chemical nature of the polymers, their molecular symmetry, and structural regularity or irregularity. Twaron fiber is highly crystalline due to the presence of bulky aromatic ring in the polymer backbone. Bulk pendant groups or short chain branches of different lengths hinder molecular packing and hinder crystallization. After fluorination, the fluorine group introduced into the polymer chain may remain as a pendant group and reduce the crystallinity.

The infrared spectroscopy of the fiber is shown in Figure 3. The strong band at 3315 cm^{-1} is the *N*-H stretching vibration. The band at 3038 cm^{-1} is due to C—H stretching of the aromatic compound. The bands at 1650–1651 cm^{-1} and 1538–1539 cm^{-1} are the so-called ν(C=O) and ν(C—N) stretching frequency of amide bands. Because of their constant position and strong intensities, they are characteristic of amides. The amide band consists mostly of the ν(C=O) and ν(C—N) stretches, and it also involves contributions of the ν (*N*-H) bending vibration. The

TABLE III
IR Peak Assignment of Nonfluorinated [TW] and Fluorinated [TWF] Twaron Fiber

Nonfluorinated Twaron fiber (TW)	Fluorinated Twaron fiber (TWF)	Peak assignment
3315	3317	ν (N—H)
3046	3038	ν (C—H)
1651	1651	ν (C=O) of amide band
–	1010	ν (C—F)
1106	1113	ν (C—N)
727	727	CH_2 rocking

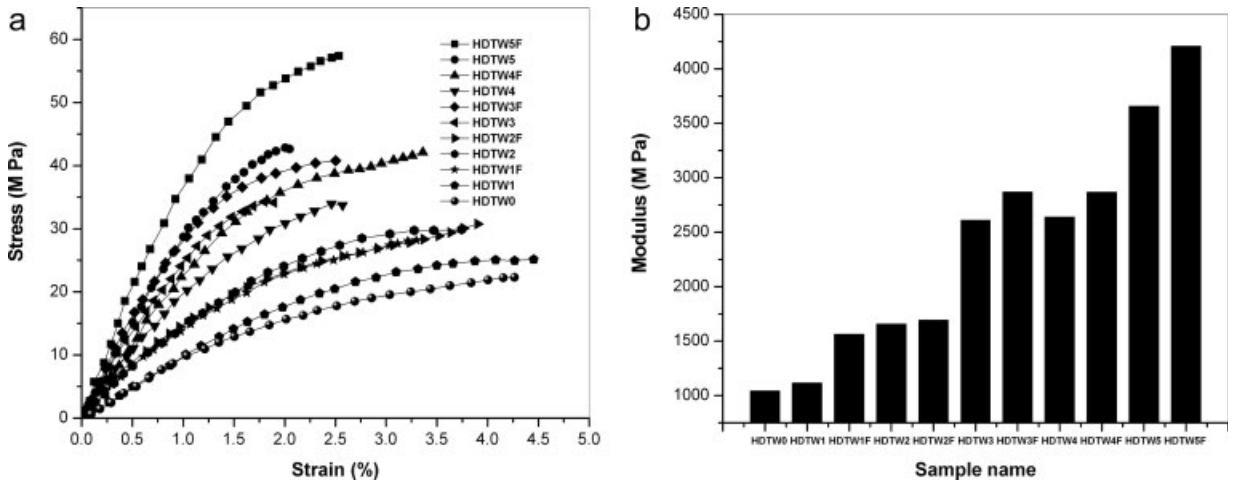

Figure 4 (a) Stress–strain plot of the virgin matrix [HDTW0] and the composites. (b) Plot of modulus of the virgin matrix [HDTW0] and the composites.

series of bands below 1500 cm^{-1} concern —C—H (1440 cm^{-1}), —CH_2 (1388 cm^{-1}), and ν(C—N) (1110 cm^{-1}) modes. The band at 723 cm^{-1} is the CH_2 rocking vibration. Some important changes occur in the infrared spectra of Twaron fiber after fluorination. The frequency at 1010 cm^{-1} is a characteristic frequency of the C—F bond. The C—F stretching frequency is absent in case of nonfluorinated fiber but appears in the fluorinated fiber. All other peak values remain almost at the nearly same position in both the cases i.e., before and after surface fluorination but fluorination of the fiber is evident from the appearance of a peak at around 1010 cm^{-1}. The probable peak values of different bonds are given in Table III.

Composite characterization

The mechanical properties of high-density polyethylene and Twaron fiber composites systems are summarized as a stress–strain curve in Figure 4(a,b) shows the plot of modulus and EB (%). The values of tensile strength, modulus and elongation at break are given in Table IV (see also Figs. 5 and 6). Polyethylene with no reinforcement shows the lowest tensile strength and modulus while also showing a higher elongation at break. The mechanical test revealed an increase in the tensile strength, modulus, and reduced elongation at break with the increase of fiber loading. It is often observed that the increase in fiber content leads to an increase in the strength and modulus,[29,30] and also in the toughness if the matrix has low toughness.[31] It is also observed that the tensile strength and modulus is higher in case of fluorinated fiber composites indicate that better mechanical interlocking between the modified fiber and the matrix takes place which is also responsible for improve fiber matrix adhesion.

The SEM micrograph of tensile fractured specimens of modified and nonmodified fiber composites is depicted in Figure 7. It is observed that the nonmodified fiber composites shows extensive fiber pullouts with wide gaps between the fibers debonded from the matrix. This confirms the weak interfacial adhesion between the nonmodified fiber and the matrix. Evidence of improved adhesion between the fiber and the matrix is observed when the fiber is fluorinated. In case of the fluorinated fiber composites, fibers are well bonded to the HDPE matrix. It is also clear from the SEM micrograph that there is a homogeneous distribution of fibers in the high density polyethylene matrix. It is well known that the homogeneous dispersion of filler in the polymer matrix is one of the conditions for a composite to show good mechanical strength reinforcement because in homogeneities can lead to structural defects in the composite material.

Infrared spectroscopic study (Fig. 8) was carried out from the range of 4000–500 cm^{-1} to investigate bond formation between the matrix and the reinforcing agent. The absorption at $\sim$ 719 cm^{-1} is due to

TABLE IV
Mechanical Properties of the Prepared Samples

Sample name	Tensile strength (MPa)	Modulus (MPa)
HDTW0	22.40	1043
HDTW1	24.24	1116
HDTW2	29.76	1567
HDTW3	34.14	2611
HDTW4	34.74	2639
HDTW5	42.87	3658
HDTW1F	28.04	1565
HDTW2F	30.71	1692
HDTW3F	41.26	2869
HDTW4F	42.09	2867
HDTW5F	57.30	4209

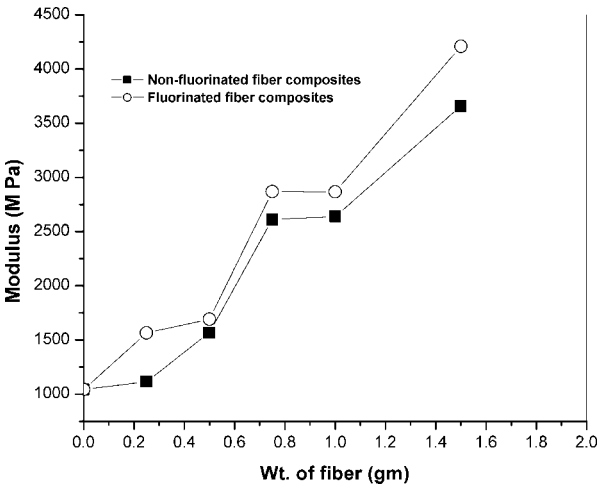

Figure 5 Plot of modulus as a function of fiber content (g).

—CH_2 rocking, absorption at 1015 cm^{-1} is due to C—F stretching frequency which is present only in the fluorinated fiber composites, the absorption at $\sim$ 2800–2900 cm^{-1} is due to C—H stretching vibration which is present in all the samples. The peak at $\sim$ 3600 and 1650 cm^{-1} are due to the stretching frequency of the -NH_2 and C=O bond of the aromatic amide compound.

X-ray Diffraction (XRD) study of the composites was also carried out. From the XRD plot, the percentage of crystallinity was calculated (see Table V, Fig. 9) using the following equation. Percent crystallinity (X_c) = $I_c \times 100/I_c + I_a$, where I_a and I_c are the area under the curve for amorphous and crystalline regions, respectively. It is shown that the crystallinity is minimum where no reinforcing agents are present and the percent crystallinity of the composites increased upto 5 wt % of fiber (both modified and nonmodified fiber) which can be explained in terms of the enhanced mobility of HDPE macromolecular chains, leading to better alignment of the crystal lattice. As the concentration of the fiber increased further, the fiber started to act as a restriction site for the HDPE segments, obstructing them from obtaining a highly ordered spherulite structure, and thus the percentage crystallinity again decreased. Crystallinity is increased in fluorinated fibers composites compared to the nonfluorinated fiber composites. This behavior is expected from the stress–strain behavior of the composite system. The XRD plots are given in Figure 10.

To see the effect of nonfluorinated and fluorinated Twaron fiber incorporation on the thermal stability of HDPE, the thermogravimetric (TG) study was conducted. The TG curves of the composites obtained at a heating rate 10°C/min in air and are shown in Figure 11 and respective parameters are tabulated in Table VI (see also Fig. 12). To avoid any ambiguity, the onset degradation temperature has been defined as the temperature at which polymer lost 1% of its weight. From the thermogram, it is observed that degradation starts at higher temperature for all Twaron/HDPE composites than pure HDPE. This enhancement in onset degradation temperature is more pronounced in case of fluorinated Twaron/HDPE composites. This extent of enhancement of thermal stability of the fluorinated Twaron/HDPE composites is may be due to the incorporation of the functional groups (during fluorination some radicals are formed) on to the Kevlar surface resulting good compatibility between two polymeric species. Moreover, it is known that crystalline polymer is thermally more stable than its amorphous counter part due to energy input required overcoming both intermolecular and intermolecular forces. It is important to point out that the extent of more interaction in case of fluorinated Twaron/HDPE composites due to more functional groups of fluorinated Twaron fiber can be responsible for a higher thermal stability of the fluorinated Twaron fiber reinforced composite.

DSC measurements were performed to characterize the thermal behavior of the samples. The results of the DSC heating and cooling scans of the composites are shown in Figure 13 and the corresponding parameters, melting temperature (T_m), crystallization temperature (T_c), heat of fusion (ΔH_f), and percent crystallinity (X_c) are tabulated in Table VII (see also Figs. 14–16). From DSC analysis, it was observed that the melting temperature of pure sample was 135°C. It was also observed that the position of the peak shifts towards higher temperature and the shifting is higher for fluorinated fiber composites. A marked increase of the crystallization peak temperature can be observed when the fibers are incorporated in the polymer matrix and this increment is

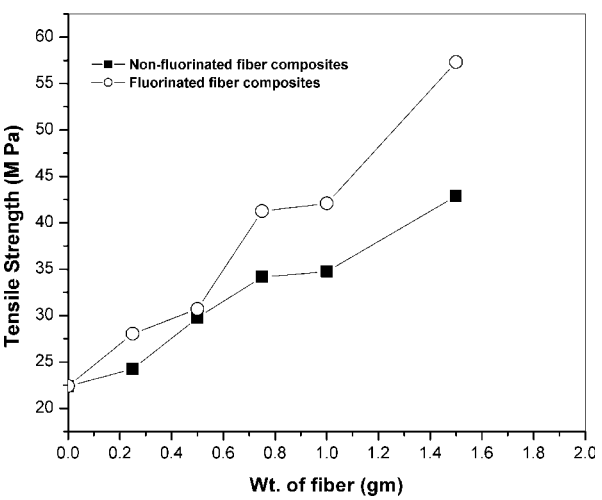

Figure 6 Plot of TS as a function of fiber content (g).

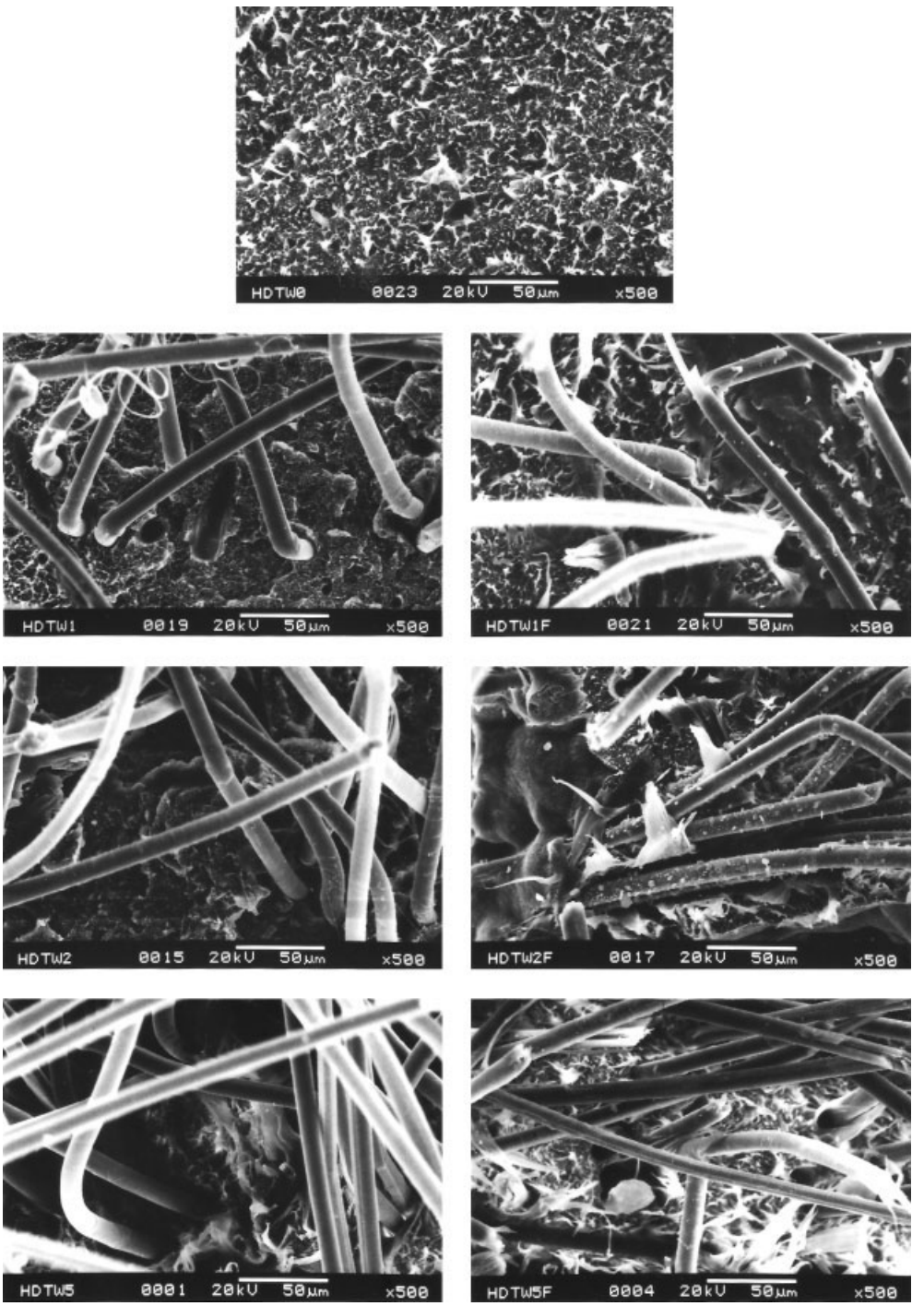

Figure 7 SEM micrograph of broken sample of virgin [HDTW0] and the nonmodified [HDTW1, HDTW2, HDTW5] and the modified fiber composites [HDTW1F, HDTW2F, HDTW5F].

more significant when the fibers are fluorinated. Crystallization peaks shift to the higher temperature side in case of all Twaron/HDPE composites. This may be due to the nucleating effect of the fibers into the HDPE matrix that supports the increasing crystallization.

It is clear from Figure 9 and Table VII that the addition of Twaron fiber to HDPE results in an increase in X_c and T_c of the PP matrix. This can be explained as due to the nucleating ability of Twaron fiber for the crystallization of HDPE. As the amount of the added fiber increases, T_c also is found to increase. T_c and enthalpy of crystallization (ΔH_c) of the PP phase increase on the addition of Twaron fiber, indicating that fibers accelerate the crystallization process. The T_c and the heat of crystallization of

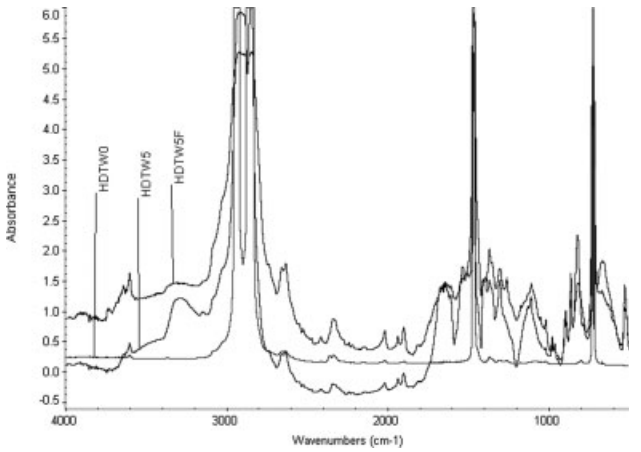

Figure 8 FTIR spectrum of Virgin matrix [HDTW0] and the composites [HDTW5, HDTW5F].

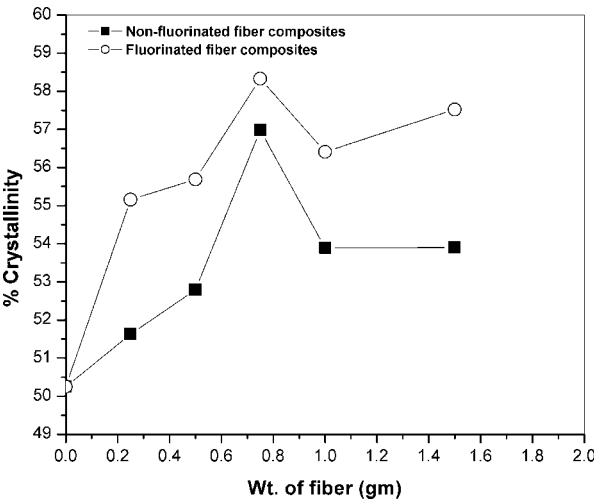

Figure 9 Plot of percent crystallinity as a function of fiber content (g).

the PP phase is further increased by the addition of chemically treated fibers (fluorinated fiber), which further favors the crystallization process. It is observed that the addition of Twaron fiber to HDPE causes only a marginal effect on T_m and no correlation of the results with the fiber content can be established. However, in the case of chemically treated composites, T_m changes appreciably, as is evidenced from Figure 9 and Table VII. As a result of fiber surface modification by chemical treatments, the compatibility between the fiber and PP matrix is increased favoring interaction between the fiber and HDPE. As the amount of fiber increases, crystallinity too increases because the fiber surface acts as nucleation sites for the crystallization and the partial crystalline growth of HDPE. It may be assumed that the nucleating effect contributes considerably to the occurrence of transcrystalline layer (TCLs) around the fibers when a specimen of the HDPE/Twaron fiber composite is cooled from the melt. Wang and Liu[32] proposed that roughness on the fiber surface enhance the formation of TCLs. After fluorination of fiber the fiber surface becomes rough and the roughness on fiber surface favors the formation of TC layers.

To study the effects produced by the fluorination of the base polymer and the composites, the surface energy of the prepared samples was evaluated from the contact angle measurements. Although the surface energy cannot be measured directly, different indirect methods have been proposed in the literature.[33,34] In this work, the geometric-mean[34–36] approximations were used to get the dispersive and the nondispersive contributions to the total surface energy of the base, modified, and the unmodified PE composites. These expressions will be used here only to compare the effects produced in the surface fluorination. The surface energy of different samples is given in Table VIII and Figure 17. From surface

TABLE V
Percentage Crystallinity of the Virgin Matrix and the Composites

Sample name	Crystallinity (%)
HDTW0	50.25
HDTW1	51.63
HDTW2	52.79
HDTW3	56.98
HDTW4	53.89
HDTW5	53.90
HDTW1F	55.16
HDTW2F	55.69
HDTW3F	58.33
HDTW4F	56.41
HDTW5F	57.52

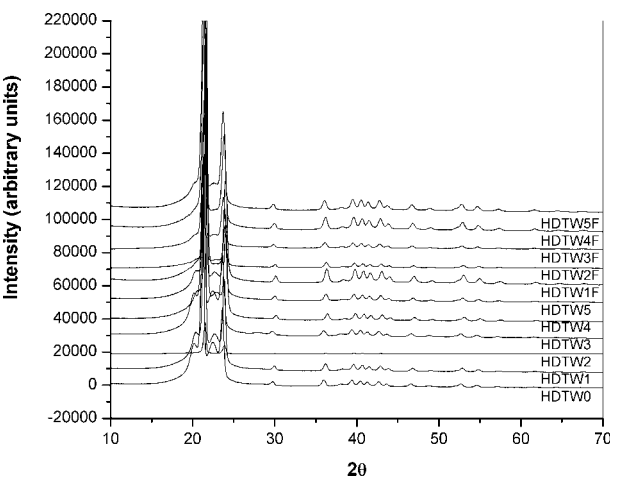

Figure 10 XRD plot of the virgin [HDTW0] and the nonmodified [HDTW1, HDTW2, HDTW3, HDTW4, HDTW5] and the modified fiber composites [HDTW1F, HDTW2F, HDTW3F, HDTW4F, and HDTW5F].

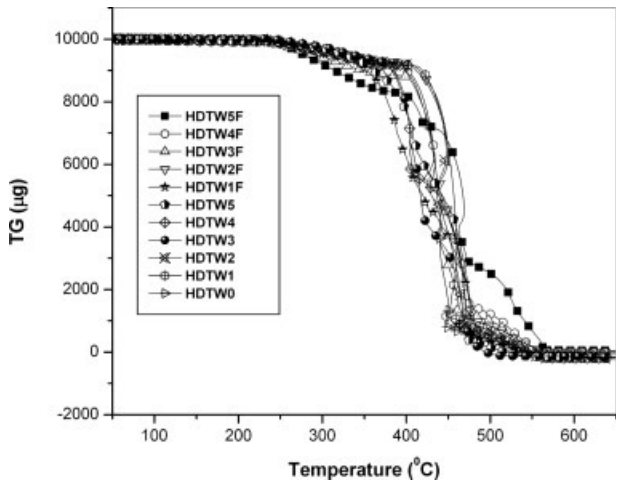

Figure 11 Thermo gravimetric (TG) plot of the virgin [HDTW0] and the composites.

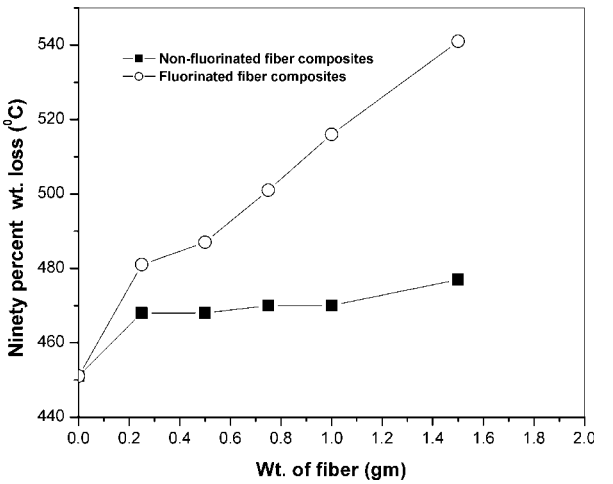

Figure 12 Plot of $T_{90\%}$ as a function of fiber content (g).

TABLE VI
Weight Loss Starting temperature and 90% Decomposition Temperature ($T_{90\%}$) Obtained from TGA

Sample name	Wt. loss started at (°C)	$T_{90\%}$ (°C)
HDTW0	262	451
HDTW1	260	468
HDTW2	250	468
HDTW3	263	470
HDTW4	262	470
HDTW5	272	477
HDTW1F	272	481
HDTW2F	255	487
HDTW3F	253	501
HDTW4F	255	516
HDTW5F	252	541

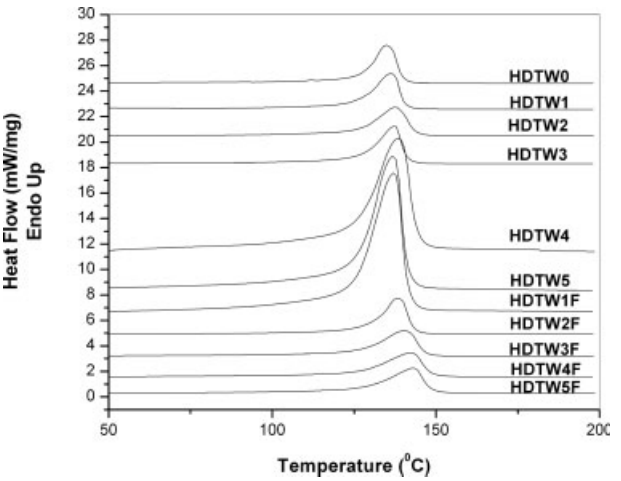

Figure 13 Melting endotherm of the virgin matrix [HDTW0] and the composites.

TABLE VII
The Results of the DSC Heating and Cooling Scans of the Virgin Matrix and the Composites

Sample name	Melting temperature, T_m (°C)	Heat of fusion, ΔH_m (J/g)	Crystallization temperature, T_c (°C)	Percent crystallinity, X_c
HDTW0	135.0	164.6	108.0	56.2
HDTW1	136.0	165.8	109.0	58.0
HDTW2	136.5	167.7	110.5	60.1
HDTW3	137.0	166.8	111.8	61.2
HDTW4	138.0	168.1	112.6	63.1
HDTW5	136.5	170.2	113.0	66.8
HDTW1F	137.0	169.7	110.5	59.4
HDTW2F	137.0	170.5	112.5	61.1
HDTW3F	139.0	170.8	113.7	62.7
HDTW4F	142.0	173.4	114.0	65.1
HDTW5F	142.0	179.3	115.0	70.3

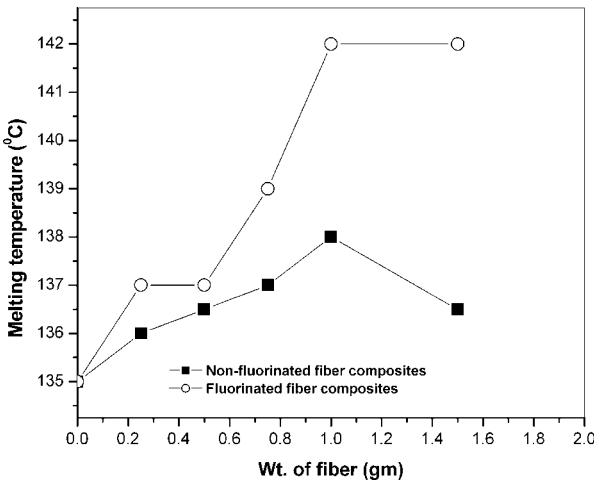

Figure 14 Plot of melting temperature as a function of fiber content (g).

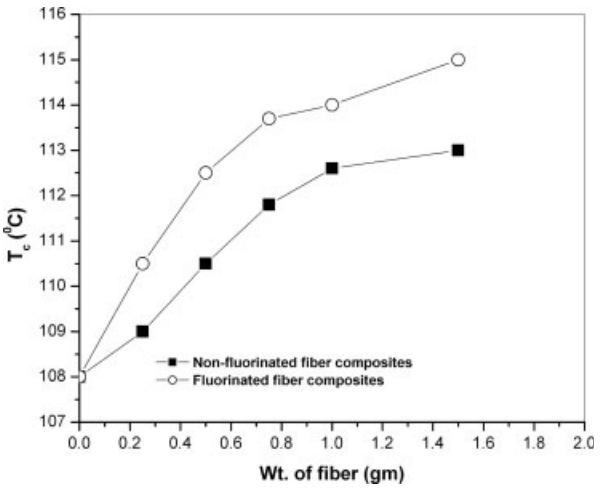

Figure 15 Plot of T_c as a function of fiber content (g).

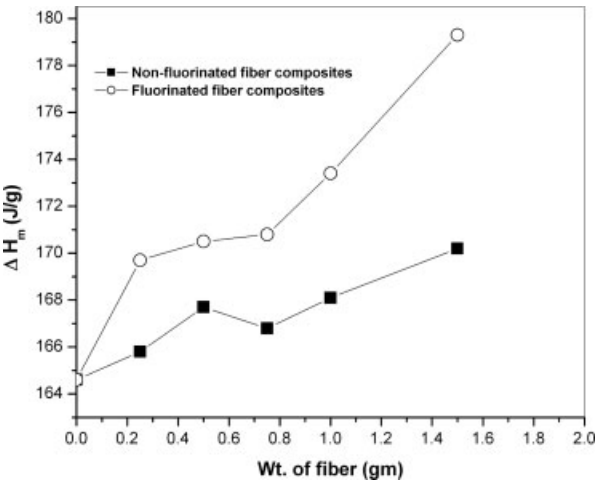

Figure 16 Plot of ΔH_m as a function of fiber content (g).

TABLE VIII
Surface Energy of the Virgin Matrix and the Composites Obtained from Contact Angle Measurement

Sample name	Surface energy (mN/m)
HDTW0	21.11
HDTW1	22.91
HDTW2	22.91
HDTW3	24.30
HDTW4	26.47
HDTW5	24.91
HDTW1F	26.89
HDTW2F	35.50
HDTW3F	35.63
HDTW4F	36.13
HDTW5F	36.80

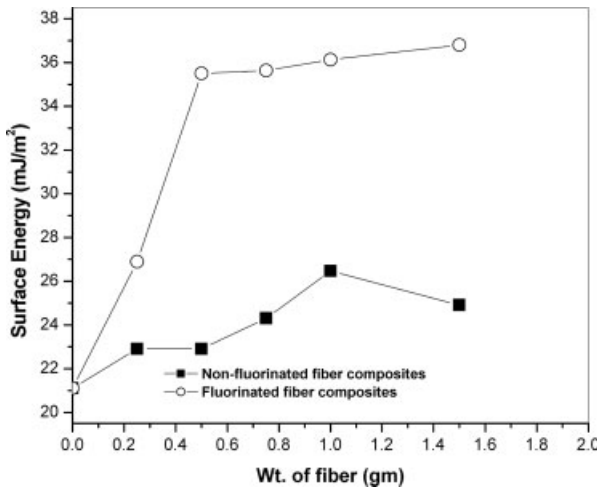

Figure 17 Plot of Surface energy as a function of fiber content (g).

energy analysis, it is observed that the surface energy is maximum for fluorinated fiber composites.

CONCLUSIONS

High density polyethylene and Twaron fiber (non-fluorinated and fluorinated) fiber composites were compounded by solution method. From the different characterization and result analysis of both the nonfluorinated and fluorinated composites it can be concluded that modified (fluorinated) fiber composites are better in strength, thermally more stable, and better wetting properties. From the view point of application, fluorinated fiber composites have higher TS, EB, and higher modulus value, in addition with the highest surface energy. The barrier properties, friction coefficient, adhesion properties, etc. for surface fluorinated composites are being studied.

References

1. Yue, C. Y.; Sui, G. X.; Looi, H. C. Compos Sci Technol 2000, 60, 421.
2. Andrews, M. C.; Day, R. J.; Hu, X; Young, R. J. Compos Sci Technol 1993, 48, 255.
3. Pi'etrement, O.; Troyon, M. J Colloid Interface Sci 2000, 226, 166.
4. Nardin, M.; Schultz, J. Compos Interface 1993, 1, 172.
5. Sheu, G. S.; Shyu, S. S. J Adhesion Sci Technol 1994, 8, 1027.
6. Dilsiz, N.; Ebert, E.; Weisweiler, W.; Akovali, G. J Colloid Interface Sci 1995, 170, 241.
7. Lin, T. K.; Wu, S. J.; Lai, J. G.; Shyu, S. S. Compos Sci Technol 2000, 60, 1873.
8. Yue, C. Y.; Padmanabhan, K. Compos B 1999, 30, 205.
9. Park, S. J.; Park, B. J. J Mater Sci Lett 1999, 18, 47.
10. Park, S. J.; Kim, M. H. J Mater Sci 2000, 35, 1901.
11. Smith, R. P.; Li, D.; Francis, D. W.; Chappuis, J.; Neumann, A. W. J Colloid Interface Sci 1993, 157, 478.
12. Rajalingam, P.; Sharpe, J.; Baker, W. E. Rubber Chem Technol 1993, 66, 664.
13. Vacearo, E.; Dibenedetto, A. T.; Huang, S. J. J Appl Polym Sci 1997, 63, 275.
14. Oromehie, A. O.; Hashemi, S. A. Polym Int 1997, 42, 117.
15. Elnesr, E. M. J Appl Polym Sci 1997, 63, 377.
16. Li, J.; Naga, K.; Ohzawa, Y.; Nakajima, T.; Shames, A. P.; Panich, A. I. J Fluorine Chem 2005, 126, 265.
17. Li, J.; Ohzawa, Y.; Nakajima, T.; Iwata, H. J Fluorine Chem 2005, 126, 1028.
18. Fukutsuka, T.; Hasegawa, S.; Matsuo, Y.; Sugie, Y.; Abe, T.; Ogumi, Z. J Power Sources 2005, 146, 151.
19. Matsumoto, K.; Li, J.; Ohzawa, Y.; Nakajima, T.; Mazej, Z.; Žemva, B. J Fluorine Chem 2006, 127, 1383.
20. Kharitonov, A. P.; Taege, R.; Ferrier, G.; Teplyakov, V. V.; Syrtsova, D. A.; Koops, G. H. J Fluorine Chem 2005, 126, 251.
21. Kharitonov, A. P.; Kharitonov, L. N.; Moslevin, Y. L.; Teplyaleor, V. V.; Syrstova, D. A.; Koops, G. H.; Kemperman, A. P. J.; Singh, R. P. Int J Plast Technol 2003, 6, 37.
22. Kharitonov, A. P. J Fluorine Chem 2000, 103, 123.
23. Grodzinski, J. J. Prog Polym Sci 1992, 17, 361.
24. Hobbs, J. P.; Henderson, P. B.; Pascolini, M. R. J Fluorine Chem 2000, 104, 87.
25. Carstens, P. A. B.; Marais, S. A.; Thompson, C. J. J Fluorine Chem 2000, 104, 97.
26. Alexander, L. E. X-ray Diffraction Methods in Polymer Science; Wiley Interscience: New York, 1969.
27. Raychowdhury, S.; Das, C. K. Polym Compos 2000, 8, 177.
28. Na, B.; Zhang, Q.; Fu, Q.; Zhang, G.; Shen, K. Polymer 2002, 43, 7367.
29. Bijsterbosch, H.; Gaymans, R. J Polym Compos 1995, 16, 363.
30. Loan Doan, T. T.; Gao, Mader, S. L. E. Compos Sci Technol 2006, 66, 952.
31. Friedrich, K. Compos Sci Technol 1985, 22, 43.
32. Wang, C.; Liu, C. Polymer 1999, 40, 289.
33. Wu, S. Polymer Interface and Adhesion; Marcel Dekker: New York, 1982; p 17.
34. Mittal, K. L. Contact Angle, Wettability and Adhesion; VSP: Utrecht, The Netherlands, 1993.
35. Owens, D. K.; Wendt, R. C. J Appl Polym Sci 1969, 13, 1741.
36. Starostina, I. A.; Stoyanov, O. V.; Bogdanova, S. A.; Deberdeev, R. J. A.; Kurnosov, V. V.; Zaikov, G. E. J Appl Polym Sci 2001, 79, 388.